

Machine Learning for Exact Time Series Aggregation in Generation Expansion Planning with Energy Storage

Jakub Rybka, Luca Santosuosso, Thomas Klatzer and Sonja Wogrin

Institute of Electricity Economics and Energy Innovation

Research Center ENERGETIC

Graz University of Technology

Graz, Austria

{j.rybka, luca.santosuosso, thomas.klatzer, wogrin}@tugraz.at

Abstract—This paper investigates a generation expansion planning (GEP) problem encompassing renewable, thermal, and storage technologies while simultaneously optimizing market participation, operational expenditures, and capital investment. To alleviate the computational burden of the GEP model, we propose a novel iterative time series aggregation (TSA) method that constructs a temporally aggregated counterpart of the original full-scale GEP model. Unlike traditional TSA methods, which are purely heuristic, our method enables the assessment of the optimality gap between the aggregated and full-scale models. Moreover, by leveraging machine learning–based estimates of the GEP model marginal costs, the algorithm guides TSA to construct an aggregated model that preserves the active constraints of its full-scale counterpart, which has been shown to yield exact temporal aggregation. Numerical results show that incorporating estimated marginal costs as clustering features substantially improves the quality of temporal aggregation compared with traditional TSA methods that rely solely on input data analysis.

Index Terms—Energy storage, exact time series aggregation, generation expansion planning, machine learning

I. INTRODUCTION

The generation expansion planning (GEP) problem is a classical optimization problem in power systems, focused on determining the optimal mix and sizing of power generation units to satisfy projected energy demand [1]. Historically, GEP has been primarily addressed by centralized system planners [2]. However, in the context of liberalized electricity markets and increasing decentralization, this problem has gained renewed relevance for generation companies and emerging actors such as virtual power plants [3], whose objectives extend beyond cost minimization to the strategic design of an energy portfolio that maximizes profitability [4] while participating in multiple electricity markets [5].

The GEP problem is typically formulated over long-term planning horizons, often spanning multiple years [6]. Furthermore, the growing penetration of variable renewable energy

(VRE) sources and flexible units, such as energy storage systems, necessitates the explicit modeling of short-term operational dynamics to accurately capture the system evolution [7]. As a result, GEP often translates into large-scale, high-temporal-resolution optimization models that can become computationally demanding or even intractable [8].

To mitigate this computational challenge, time series aggregation (TSA) has emerged as a widely adopted approach [9]. TSA reduces the full-scale GEP model to an aggregated model defined over a reduced set of representative time steps or clusters [10]. When the number of representative steps is significantly smaller than the original time steps in the full-scale model, solving the aggregated model yields a significant computational advantage over its full-scale counterpart.

TSA methods are generally classified as *a priori* or *a posteriori* [9]. Traditional *a priori* methods perform TSA based solely on the statistical features of the input time series to the GEP model, typically employing standard clustering techniques such as K-Means [11], K-Medoids [12], or hierarchical clustering [13]. However, accurately representing the GEP input space does not guarantee an accurate representation of its output space, meaning that the aggregated model output may still deviate significantly from that of the full-scale model [14].

Conversely, a *posteriori* TSA leverages structural information from the full-scale model to guide temporal aggregation. For example, historical optimization runs can be used to estimate optimal decision variable values, which are then employed as clustering features [15]. Alternatively, daily sub-problems may be solved to approximate the distribution of investment costs, which subsequently serve as features in K-Medoids [16] or K-Means [17] clustering, rather than relying solely on input data analysis. A related approach extracts information from an initial *a priori* aggregated model to identify and emphasize extreme periods in the final aggregation [18].

Notably, previous research has demonstrated that a *posteriori* TSA methods capable of constructing an aggregated model that preserves the active constraints of the full-scale model achieve **exact** temporal aggregation [19]; that is, the aggregated model yields the same optimal objective function

Funded by the European Union (ERC, NetZero-Opt, 101116212). Views and opinions expressed are however those of the authors only and do not necessarily reflect those of the European Union or the European Research Council. Neither the European Union nor the granting authority can be held responsible for them.

value as the original full-scale model. This theoretical result has been further extended to optimization models incorporating storage intertemporal constraints, where TSA is further challenged by the need to maintain temporal chronology [20]. In practical applications, however, it is unrealistic to assume prior knowledge of the GEP model's active constraints. Consequently, a critical research gap persists in the development of a practical a posteriori TSA method capable of constructing an aggregated model that approximates the active constraints of its full-scale counterpart, targeting exact temporal aggregation while preserving chronology under intertemporal constraints.

This paper addresses this research gap through the following key contributions:

- We formulate a GEP model that accounts for both capital investment and operational performance in the energy market while incorporating storage constraints. Building on this formulation, we propose a machine learning (ML) framework to estimate the marginal costs of the GEP model, i.e., the dual variables associated with the energy balancing constraints. These estimates are then used as clustering features to construct an aggregated model that preserves the active constraints of its full-scale counterpart, thereby explicitly targeting exact TSA.
- The proposed ML framework, which yields marginal cost estimates, is embedded within a novel *a posteriori* TSA-based solution algorithm that provides explicit bounds on the approximation error introduced by the temporal aggregation procedure, thereby offering a clear and practical performance guarantee to the decision-maker.
- We benchmark the proposed TSA-based solution algorithm against state-of-the-art methods, including both traditional a priori TSA and recent a posteriori alternatives, to assess its potential for reducing computational complexity while yielding improved accuracy.

Finally, the performance of the proposed algorithm is validated using real-world Austrian hourly data on VRE capacity factors, energy demand, and energy prices for the year 2024.

The remainder of the paper is structured as follows. Section II introduces the proposed methodology. Section III presents the numerical results, and Section IV concludes the paper.

II. METHODOLOGY

This section presents the proposed methodology. Subsection II-A describes the aggregated GEP model. The ML framework and solution algorithm are detailed in Subsections II-B and II-C, respectively.

A. Aggregated Model

Let \mathcal{T} , indexed by $t \in \{1, \dots, T\}$, denote the temporal horizon of the GEP problem. A traditional full-scale formulation is provided in Appendix A. As \mathcal{T} grows, the full-scale model may become computationally intractable. To address this, we introduce an aggregated GEP model defined over a reduced set of representative time steps \mathcal{R} , indexed by $r \in \{1, \dots, R\}$.

Let $\mathcal{T}_r \subseteq \mathcal{T}$ denote the set of consecutive time steps in \mathcal{T} associated with representative step r , with cardinality $W_r :=$

$|\mathcal{T}_r|$. Moreover, let \mathcal{G} and \mathcal{S} denote the sets of generators, and storage units, respectively, indexed by g and s . All sets are indexed starting from 1.

The charging and discharging efficiencies of the s -th storage unit are denoted by η_s^c and η_s^d , respectively. We denote by \bar{E}_s , \bar{P}_s^d , \bar{P}_s^c , and \underline{E}_s the maximum state of charge (MWh), discharging capacity (MW), charging capacity (MW), and minimum state of charge (MWh) of the s -th storage unit, respectively. The investment and operational costs of g are denoted by C_g^{inv} (€/MW) and C_g (€/MWh), respectively. The penalty for non-supplied energy and the cost of discharging are C_r^{ns} (€/MWh) and C_s^d (€/MWh), respectively. We denote by \bar{B} the investment budget (€). Finally, Δ denotes the time resolution (h) of the GEP problem.

Let \hat{x}_g denote the capacity (MW) of generator g , $\hat{p}_{g,r}$ its power output (MW), and \hat{e}_r^{ns} the non-supplied energy (MWh) at the representative time step r . We denote by \hat{o}_r the energy (MWh) sold to the market at the representative time step r . Moreover, $\hat{e}_{s,r}$ denotes the state of charge (MWh) of the storage unit s at the representative time step r , while $\hat{p}_{s,r}^c$ and $\hat{p}_{s,r}^d$ (MW) denote its charging and discharging power, respectively. We introduce an auxiliary variable $\hat{e}_{s,0}$ to represent the initial state of charge of the storage unit s .

For all $r \in \mathcal{R}$, the aggregated input time series, denoted by $\hat{F}_{g,r}$, \hat{D}_r , and $\hat{\pi}_r$, are given by:

$$\hat{F}_{g,r} := \sum_{t \in \mathcal{T}_r} \frac{F_{g,t}}{W_r}, \quad \hat{D}_r := \sum_{t \in \mathcal{T}_r} \frac{D_t}{W_r}, \quad \hat{\pi}_r := \sum_{t \in \mathcal{T}_r} \frac{\pi_t}{W_r},$$

where $F_{g,t}$, D_t , and π_t denote capacity factors (p.u.), demand (MWh), and market signal time series (€/MWh), respectively.

We group the decision variables of the aggregated model into the set $\hat{\mathbf{z}}$ as follows:

$$\hat{\mathbf{z}} := \left\{ \hat{x}_g, \hat{p}_{g,r}, \hat{p}_{s,r}^d, \hat{p}_{s,r}^c, \hat{e}_r^{\text{ns}}, \hat{e}_{s,r}, \hat{o}_r \right\}_{g \in \mathcal{G}, r \in \mathcal{R}, s \in \mathcal{S}}, \quad (1)$$

while the aggregated objective function is defined as

$$\hat{f}(\hat{\mathbf{z}}) := \sum_{g \in \mathcal{G}} C_g^{\text{inv}} \hat{x}_g + \sum_{r \in \mathcal{R}} W_r \left(\Delta \sum_{g \in \mathcal{G}} C_g \hat{p}_{g,r} + \Delta \sum_{s \in \mathcal{S}} C_s^d \hat{p}_{s,r}^d + C_r^{\text{ns}} \hat{e}_r^{\text{ns}} - \hat{\pi}_r \hat{o}_r \right). \quad (2)$$

The **aggregated GEP model** is formulated as follows:

$$\min_{\hat{\mathbf{z}} \geq 0} \hat{f}(\hat{\mathbf{z}}) \quad (3a)$$

$$\text{s.t.} \quad \sum_{g \in \mathcal{G}} \hat{p}_{g,r} \Delta + \sum_{s \in \mathcal{S}} (\hat{p}_{s,r}^d - \hat{p}_{s,r}^c) \Delta + \hat{e}_r^{\text{ns}} - \hat{o}_r = \hat{D}_r, \forall r, \quad (3b)$$

$$\hat{p}_{g,r} \leq \hat{F}_{g,r} \hat{x}_g, \quad \forall g, \forall r, \quad (3c)$$

$$\hat{e}_{s,r} = \hat{e}_{s,r-1} + \left(\eta_s^c \hat{p}_{s,r}^c - \frac{\hat{p}_{s,r}^d}{\eta_s^d} \right) \Delta W_r, \quad \forall s, \forall r, \quad (3d)$$

$$\hat{e}_{s,0} = \hat{e}_{s,R} = \underline{E}_s, \quad \forall s, \quad (3e)$$

$$\underline{E}_s \leq \hat{e}_{s,r} \leq \bar{E}_s, \quad \forall s, \forall r, \quad (3f)$$

$$\hat{p}_{s,r}^c \leq \bar{P}_s^c, \quad \forall s, \forall r, \quad (3g)$$

$$\hat{p}_{s,r}^d \leq \bar{P}_s^d, \quad \forall s, \forall r, \quad (3h)$$

$$\sum_{g \in \mathcal{G}} C_g^{\text{inv}} \hat{x}_g \leq \bar{B}. \quad (3i)$$

In (3), objective (3a) scales operational costs by W_r , while (3b) ensures energy balance. Generation limits are enforced by (3c), and storage dynamics by (3d)–(3f). Finally, (3g), (3h), and (3i) bound charging, discharging, and cumulative investment. Notably, when $\mathcal{R} = \mathcal{T}$, the model is equivalent to the full-scale formulation provided in Appendix A.

B. Machine Learning for Marginal Cost Estimation

Klatzer et al. [20] demonstrate that aggregating consecutive time steps with identical active constraints yields **exact** temporal aggregation. Because these constraints are unknown a priori, we propose a **marginal-cost-based (MCB) TSA method**. This method employs an ML framework to estimate full-scale marginal costs as clustering features, ensuring the aggregated model (3) preserves the active constraints of the full-scale model (7).

The proposed ML framework takes the GEP input time series $\Omega^{\mathcal{T}}$, comprising capacity factors, demand, and energy prices, and estimates its unknown true distribution $P(\Omega^{\mathcal{T}})$ via Kernel Density Estimation [21], yielding the estimate $\bar{P}(\Omega^{\mathcal{T}})$. An artificial time series $\Omega^{\mathcal{K}}$ is generated by drawing K samples from $\bar{P}(\Omega^{\mathcal{T}})$ and used to solve a reduced version of the full-scale GEP model (7), defined over \mathcal{K} instead of \mathcal{T} . The outputs of this reduced GEP model are then used to train a Random Forest classifier [22], which is subsequently employed to generate estimates of the marginal costs $\bar{\mu}$ over the full planning horizon \mathcal{T} . The classifier is configured with $M = 100$ trees and a maximum depth of 20. The bootstrap aggregation mitigates overfitting, while the chosen depth enables the capture of marginal cost variations without sacrificing generalization. With a training complexity of $O(M \cdot K \log K)$, the computational overhead of the ML framework remains negligible compared to that of the full-scale GEP model.

The proposed ML framework is summarized as follows:

- 1) **Input:** $\Omega^{\mathcal{T}} := \{F_{g,t}, D_t, \pi_t\}_{g \in \mathcal{G}, t \in \mathcal{T}}$.
- 2) **Density estimation:** Estimate the input data distribution $\bar{P}(\Omega^{\mathcal{T}}) \approx P(\Omega^{\mathcal{T}})$ via Kernel Density Estimation [21].
- 3) **Sampling:** Draw K samples from $\bar{P}(\Omega^{\mathcal{T}})$ to generate a time series $\Omega^{\mathcal{K}} := \{\bar{P}(\Omega^{\mathcal{T}})_k\}_{k \in \mathcal{K}}$, with $K \ll |\mathcal{T}|$.
- 4) **Marginal costs extraction:** Solve the GEP model (7) for $\Omega^{\mathcal{K}}$ to obtain the marginal cost estimates $\tilde{\mu} := \{\tilde{\mu}_k\}_{k \in \mathcal{K}}$.
- 5) **Training:** Train a Random Forest [22] classifier $\mathcal{C} : \Omega^{\mathcal{T}} \rightarrow \bar{\mu}$ using the labeled pairs $(\Omega^{\mathcal{K}}, \tilde{\mu})$.
- 6) **Inference:** Predict the marginal costs $\bar{\mu} := \{\bar{\mu}_t\}_{t \in \mathcal{T}}$ for the full planning horizon \mathcal{T} using \mathcal{C} .

C. Marginal-Cost-Based Time Series Aggregation

The aggregated model (3) solution provides a lower bound (f^{LB}) to the optimal objective function value (f^*) of the full-scale model (7) [23]. Projecting the aggregated model solution onto the feasible space of (7) then yields an upper bound (f^{UB}). In Algorithm 1, this bounding procedure is combined with the ML framework to iteratively refine the aggregated

model (3) toward exact TSA, while monitoring the achieved optimality gap at each iteration.

Algorithm 1: Time Series Aggregation Guided by Marginal Cost Estimates

- Input:** $\Omega^{\mathcal{T}}, R^0, K, N^{\text{top}}, \epsilon^{\text{target}}, \bar{R}, \delta_R$.
Output: Objective function bounds f^{UB} and f^{LB} .
- 1 Predict $\bar{\mu}$ using the ML framework of Subsection II-B;
 - 2 Construct \mathcal{T}^{top} consisting of the N^{top} time steps in \mathcal{T} with the highest net demand \tilde{D}_t , calculated as in (4);
 - 3 $\mathcal{T}^- := \mathcal{T} \setminus \mathcal{T}^{\text{top}}$;
 - 4 $\{\mathcal{R}^{\text{top}}, \mathcal{T}_{\mathcal{R}^{\text{top}}}\} \leftarrow$ For each $\tilde{t} \in \mathcal{T}^{\text{top}}$, create a representative time step \tilde{r} with $\mathcal{T}_{\tilde{r}} := \{\tilde{t}\}$, then include \tilde{r} in \mathcal{R}^{top} and $\mathcal{T}_{\tilde{r}}$ in $\mathcal{T}_{\mathcal{R}^{\text{top}}}$.
 - 5 **Initialization:** $\epsilon \leftarrow +\infty, R \leftarrow R^0$;
 - 6 **while** $\epsilon > \epsilon^{\text{target}}$ **and** $R < \bar{R}$ **do**
 - 7 $\{\mathcal{R}^-, \mathcal{T}_{\mathcal{R}^-}\} \leftarrow$ Perform chronological hierarchical clustering [10], using $\{\bar{\mu}_t\}_{t \in \mathcal{T}^-}$ as clustering features, $|\bar{\mu}_t - \bar{\mu}_{t'}|$ as distance metric between consecutive time steps t and t' , and R as the desired number of representative time steps;
 - 8 $\mathcal{R} \leftarrow \mathcal{R}^- \cup \mathcal{R}^{\text{top}}$;
 - 9 $\mathcal{T}_{\mathcal{R}} \leftarrow \mathcal{T}_{\mathcal{R}^-} \cup \mathcal{T}_{\mathcal{R}^{\text{top}}}$;
 - 10 $\hat{z}^* \leftarrow$ Solve the aggregated GEP model (3) over \mathcal{R} ;
 - 11 $f^{\text{LB}} \leftarrow \hat{f}(\hat{z}^*)$; // Lower bound from the aggregated objective function (2)
 - 12 $\bar{z}^* \leftarrow$ Solve (7) with generation capacity variables fixed to their values in \hat{z}^* ;
 - 13 $f^{\text{UB}} \leftarrow f(\bar{z}^*)$; // Upper bound
 - 14 $\epsilon \leftarrow 100 \frac{(f^{\text{UB}} - f^{\text{LB}})}{f^{\text{UB}}}$; // Optimality gap
 - 15 $R \leftarrow R + \delta_R$;
-

The algorithm uses the marginal cost estimates $\bar{\mu}$ as clustering features for TSA, within the chronological hierarchical clustering algorithm of [10]. It terminates when the optimality gap ϵ , defined as the relative difference between the upper and lower bounds, falls below the target ϵ^{target} or when the maximum aggregated model size \bar{R} is reached. At each iteration, the number of representative steps R is increased from the initial value R^0 by δ_R , progressively refining the objective function bounds. To improve aggregation fidelity, full resolution is maintained for a protected set \mathcal{T}^{top} comprising the N^{top} time steps with the highest net demand. The net demand \tilde{D}_t is estimated from the generation capacities \tilde{x}_g obtained via the ML framework in Subsection II-B, as follows:

$$\tilde{D}_t = D_t - \Delta \sum_{g \in \mathcal{G}} \tilde{x}_g F_{g,t}, \quad \forall t. \quad (4)$$

The proposed Algorithm 1 exhibits two notable features. First, it provides a measure of the optimality gap achieved by the TSA method at each iteration [23], thereby offering a formal performance guarantee to the decision-maker, whereas traditional a priori TSA methods are purely heuristic. Second, it leverages structural information from the full-scale GEP

model, specifically the marginal cost estimates, to guide TSA toward exact temporal aggregation, whereas conventional a priori TSA methods rely solely on input data analysis.

III. NUMERICAL RESULTS

This section presents a performance evaluation of the proposed MCB TSA in comparison with several state-of-the-art TSA methods. In Subsection III-A, we consider a cost minimization problem in which market participation is disregarded in the GEP model, while Subsection III-B considers a GEP problem that includes market participation.

The case study relies on historical open-source data on demand, capacity factors, and energy prices in Austria for 2024, obtained from the ENTSO-E Transparency Platform [24]. These data are perturbed across 10 distinct scenarios using uniform noise drawn from the interval $[0.8, 1.2]$ to assess the sensitivity of the analyzed TSA methods to variations in the input data. The sensitivity across scenarios is reported using boxplots, where the boxes denote the interquartile range, the median is shown in blue, and the whiskers encompass all data points. Each case study includes a single storage unit with varying energy-to-power ratios (in hours), \bar{E}_s/\bar{P}_s^d , along with one renewable and one thermal generation unit.

We assume generation costs of 130, 2.5, and 1 (€/MWh) for thermal, wind, and PV units, respectively. The investment costs are 10^5 (€/MW) for thermal units and 8×10^4 (€/MW) for VRE. The non-supplied energy cost is 5×10^3 (€/MWh), and the storage discharging cost is 1.5 (€/MWh). For the storage unit, we set $\eta_s^c = 0.9$, $\eta_s^d = 0.9$, $\bar{P}_s^d = 200$ (MW), $\bar{P}_s^c = 200$ (MW), $\bar{E}_s = 0$ (MWh). The investment budget is 3×10^8 (€).

All GEP models are defined over 8,736 time steps at an hourly resolution. In Algorithm 1, we set $\epsilon^{\text{target}} = 1\%$, $\bar{R} = 900$, $R^0 = 400$, $\delta_R = 100$, $K = 500$, and $N^{\text{top}} = 100$.

To balance accuracy and computational complexity, the optimal values of K and N^{top} were determined through a sensitivity analysis. Results indicate that $K < 500$ fails to adequately capture the input time series distribution, leading to inaccurate marginal cost representations, whereas $K > 500$ yields negligible improvement. Similarly, $N^{\text{top}} < 100$ underestimates investment decisions by omitting extreme periods, while larger values provide no significant additional benefit.

The key differences between the proposed MCB TSA method and the benchmark methods are summarized in Table I. For consistency, all methods are implemented within Algorithm 1, with the adopted clustering features and techniques varying according to the specific TSA method. Specifically, [10] and [13] propose a priori TSA methods that rely solely on the input data to identify representative hours [10] or days [13]. We further compare our method with a posteriori TSA methods that exploit structural information from the GEP model through estimates of the optimal primal variable values, such as investment decisions [15] or net demand [18], whereas our method instead employs estimates of the dual information, namely the marginal costs, as clustering features.

The GEP models were solved on an Intel Xeon W5 workstation with 256 GB of RAM using Gurobi 13.0.0.

TABLE I: Comparison of the analyzed TSA methods.

Method	Clustering features	Clustering	Type of TSA method
[10]	Input data	CHC	A priori
[13]	Input data	HC	A priori
[15]	Primal variables	K-Medoids	A posteriori
[18]	Primal variables	K-Medoids	A posteriori
MCB	Dual variables	CHC	A posteriori

Legend: Chronological hierarchical clustering (CHC), hierarchical clustering (HC).

A. Cost Minimization Problem

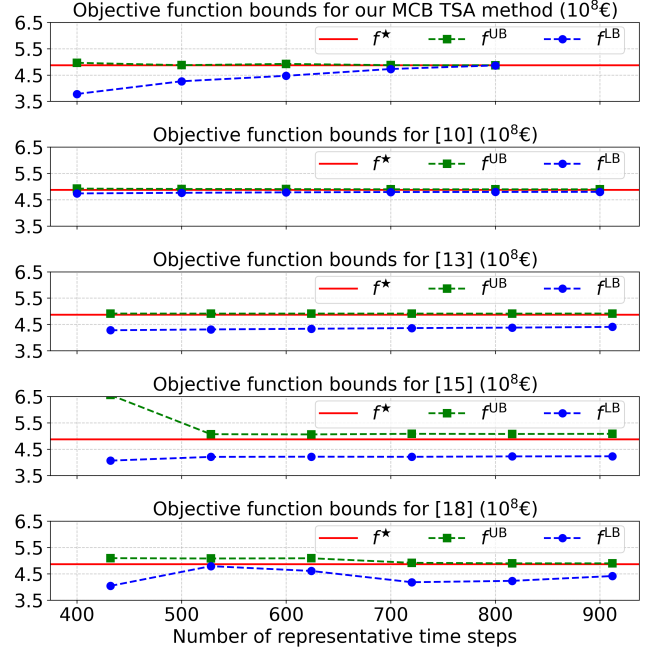
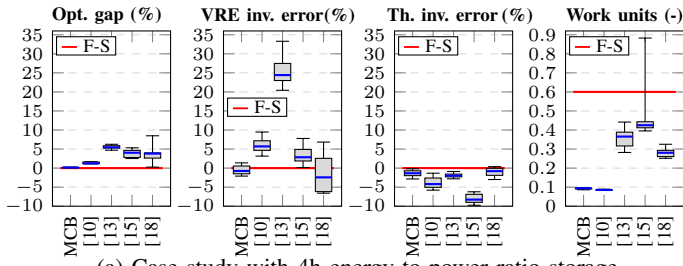


Fig. 1: Objective function bounds for a stylized cost minimization problem with a wind unit as the only VRE source and a storage unit with a 4h energy-to-power ratio.

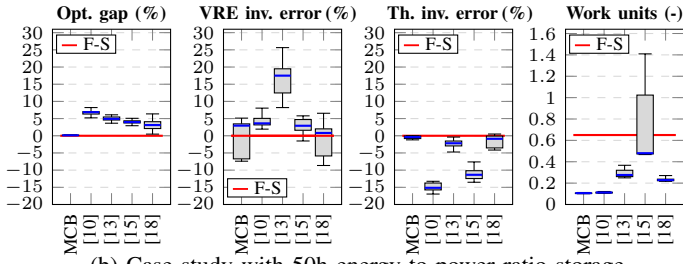
The observed objective function bounds are reported in Fig. 1. Our MCB TSA method outperforms all benchmark methods, converging to the desired optimality gap with 800 representative steps. Notably, the TSA method of [10] yields the smallest initial optimality gap (3.7%), observed at the first iteration of Algorithm 1, but fails to reach the target gap of 1%. Since our method differs from that of [10] in the clustering features employed (estimated marginal costs versus input time series), this result further underscores the effectiveness of marginal costs as proxies for exact TSA.

Figures 2 and 3 show TSA method sensitivity across 10 scenarios with uniform data perturbations. Models include either a PV (Fig. 2) or a wind unit (Fig. 3), each coupled with storage (\bar{E}_s/\bar{P}_s^d ratios of 4–50 h). Performance is evaluated model via optimality gap, solution time (work units), and VRE/thermal investment errors relative to full-scale model.

Our MCB TSA method outperforms benchmarks, reducing solution time tenfold compared to the full-scale optimization. By leveraging structural information from the full-scale model,

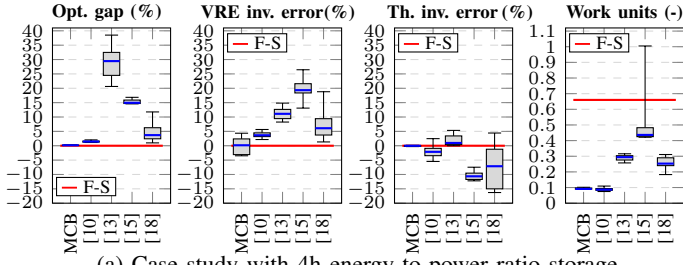


(a) Case study with 4h energy-to-power ratio storage.

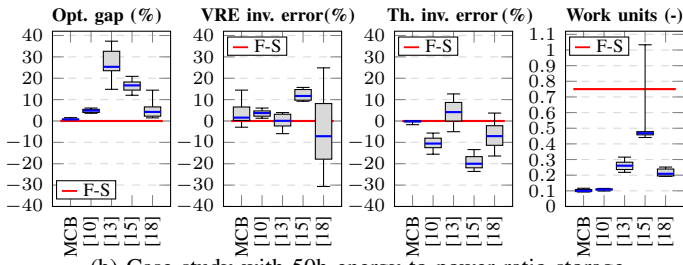


(b) Case study with 50h energy-to-power ratio storage.

Fig. 2: TSA performance relative to full-scale (F-S) optimization, with perturbed **PV** data in a cost minimization problem.



(a) Case study with 4h energy-to-power ratio storage.



(b) Case study with 50h energy-to-power ratio storage.

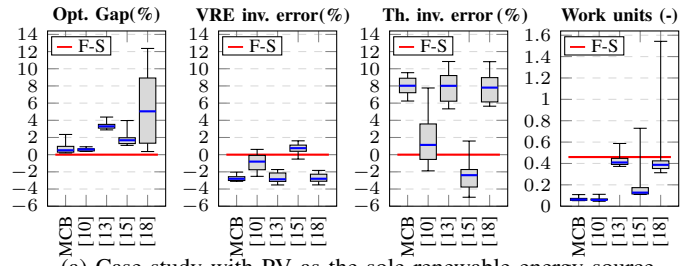
Fig. 3: TSA performance relative to full-scale (F-S) optimization, with perturbed **wind** data in a cost minimization problem.

it demonstrates superior robustness to data perturbations compared to input-dependent alternatives. Although validated on a small case study, the method generalizes to larger systems provided that marginal costs are accurately captured. Future work will focus on aggregating heterogeneous marginal costs in systems with diverse technologies and network constraints.

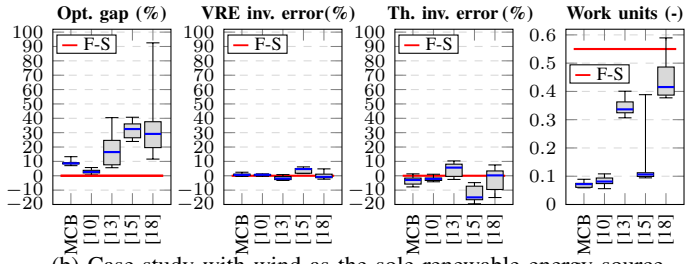
B. Market Participation Problem

This subsection presents the performance of our TSA method for a GEP model incorporating market participation.

Fig. 4 reports the performance of the analyzed TSA methods when both wind and PV capacity factor time series are per-



(a) Case study with PV as the sole renewable energy source.



(b) Case study with wind as the sole renewable energy source.

Fig. 4: TSA performance relative to full-scale (F-S) optimization, under perturbed **PV** and **wind** data for GEP with market participation and a storage unit with 4h energy-to-power ratio.

turbed with the aforementioned uniform noise. The inclusion of market prices degrades the performance of our MCB TSA method (see the optimality gaps in Fig. 4) relative to the cases illustrated in the previous subsection, as the number of distinct marginal cost values in the GEP model increases.

Our MCB TSA method maintains the lowest optimality gap, though all methods yield similar investment errors. This suggests our approach excels at capturing operational decisions, as true marginal costs are more accurately reflecting operations rather than investments. Consistent with previous results, our method reduces solution time tenfold compared to full-scale optimization.

IV. CONCLUSIONS

This paper investigates the GEP problem for a power system comprising renewable, thermal, and storage technologies, jointly optimizing market participation as well as operational and investment costs. To overcome the heuristic nature of traditional TSA procedures, we propose a novel iterative TSA method that enables the explicit assessment of the optimality gap at each iteration. Notably, the method targets exact temporal aggregation by employing ML-based estimates of the marginal costs as clustering features to construct an aggregated model that retains the same active constraints as its full-scale counterpart. Numerical results show that the proposed method outperforms existing TSA methods in solution accuracy while achieving an order-of-magnitude runtime reduction relative to traditional full-scale optimization. Future work will consider large-scale GEP problems and incorporate additional technical constraints, such as ramping and network constraints, to evaluate the applicability of the proposed MCB TSA method to a broader class of GEP models.

REFERENCES

- [1] N. E. Koltsaklis and A. S. Dagoumas, "State-of-the-art generation expansion planning: A review," *Appl. Energy*, vol. 230, pp. 563-589, Nov. 2018.
- [2] F. López-Ramos, S. Nasini, and M. H. Sayed, "An integrated planning model in centralized power systems," *Eur. J. Oper. Res.*, vol. 287, no. 1, pp. 361-377, Nov. 2020.
- [3] L. Santosousso et al., "Economic model predictive control for the energy management problem of a virtual power plant including resources at different voltage levels," in *27th Int. Conf. Electricity Distrib. (CIRED 2023)*, Rome, Italy, 2023, pp. 2044-2048.
- [4] H. Sadeghi, M. Rashidinejad, and A. Abdollahi, "A comprehensive sequential review study through the generation expansion planning," *Renew. Sustain. Energy Rev.*, vol. 67, pp. 1369-1394, Jan. 2017.
- [5] L. Santosousso, S. Camal, F. Liberati, A. Di Giorgio, A. Michiorri, and G. Kariniotakis, "Stochastic economic model predictive control for renewable energy and ancillary services trading with storage," *Sustain. Energy, Grids Netw.*, vol. 38, pp. 101373, June 2024.
- [6] C. Li, A. J. Conejo, P. Liu, B. P. Omell, J. D. Sirola, and I. E. Grossmann, "Mixed-integer linear programming models and algorithms for generation and transmission expansion planning of power systems," *Eur. J. Oper. Res.*, vol. 297, no. 3, pp. 1071-1082, Mar. 2022.
- [7] T. Levin, P. L. Blaisdell-Pijuan, J. Kwon, and W. N. Mann, "High temporal resolution generation expansion planning for the clean energy transition," *Renew. Sustain. Energy Transit.*, vol. 5, p. 100072, Aug. 2024.
- [8] L. Kotzur et al., "A modeler's guide to handle complexity in energy systems optimization," *Adv. Appl. Energy*, vol. 4, p. 100063, Nov. 2021.
- [9] M. Hoffmann, L. Kotzur, D. Stolten, and M. Robinius, "A review on time series aggregation methods for energy system models," *Energies*, vol. 13, no. 3, p. 641, Feb. 2020.
- [10] S. Pineda and J. M. Morales, "Chronological time-period clustering for optimal capacity expansion planning with storage," *IEEE Trans. Power Syst.*, vol. 33, no. 6, pp. 7162-7170, Nov. 2018.
- [11] L. Kotzur, P. Markewitz, M. Robinius, and D. Stolten, "Time series aggregation for energy system design: Modeling seasonal storage," *Appl. Energy*, vol. 213, pp. 123-135, Mar. 2018.
- [12] H. Teichgraber and A. R. Brandt, "Clustering methods to find representative periods for the optimization of energy systems: an initial framework and comparison," *Appl. Energy*, vol. 239, pp. 1283-1293, Apr. 2019.
- [13] M. Moradi-Sepahvand and S. H. Tindemans, "Capturing chronology and extreme values of representative days for planning of transmission lines and long-term energy storage systems," in *Proc. 2023 IEEE Belgrade PowerTech*, Belgrade, Serbia, 2023.
- [14] H. Teichgraber and A. R. Brandt, "Time-series aggregation for the optimization of energy systems: Goals, challenges, approaches, and opportunities," *Renew. Sustain. Energy Rev.*, vol. 157, p. 111984, Apr. 2022.
- [15] Y. Zhang, V. Cheng, D. S. Mallapragada, J. Song, and G. He, "A model-adaptive clustering-based time aggregation method for low-carbon energy system optimization," *IEEE Trans. Sustain. Energy*, vol. 14, no. 1, pp. 55-64, Aug. 2023.
- [16] M. Sun, F. Teng, X. Zhang, G. Strbac, and D. Pudjianto, "Data-driven representative day selection for investment decisions: A cost-oriented approach," *IEEE Trans. Power Syst.*, vol. 34, no. 4, pp. 2925-2936, July 2019.
- [17] C. Li, A. J. Conejo, J. D. Sirola, and I. E. Grossmann, "On representative day selection for capacity expansion planning of power systems under extreme operating conditions," *Int. J. Electr. Power Energy Syst.*, vol. 137, p. 107697, May 2022.
- [18] A. P. Hilbers, D. J. Brayshaw, and A. Gandy, "Reducing climate risk in energy system planning: A posteriori time series aggregation for models with storage," *Appl. Energy*, vol. 334, p. 120624, Mar. 2023.
- [19] S. Wogrin, "Time series aggregation for optimization: One-size-fits-all?," *IEEE Trans. Smart Grid*, vol. 14, no. 3, pp. 2489-2492, Feb. 2023.
- [20] T. Klatzer, D. Cardona-Vasquez, L. Santosousso, and S. Wogrin, "Towards exact temporal aggregation of time-coupled energy storage models via active constraint set identification and machine learning," arXiv:2504.19699, Oct. 2025.
- [21] Y. C. Chen, "A tutorial on kernel density estimation and recent advances," *Biostatistics Epidemiol.*, vol. 1, no. 1, pp. 161-187, Oct. 2017.
- [22] A. Parmar, R. Katariya, and V. Patel, "A review on random forest: An ensemble classifier," in *Int. Conf. Intell. Data Commun. Technol. Internet Things (ICICI)*, Coimbatore, India, 2018, pp. 758-763.
- [23] L. Santosousso and S. Wogrin, "Optimal virtual power plant investment planning via time series aggregation with bounded error," in *2025 IEEE PES Innov. Smart Grid Technol. Conf. Europe (ISGT Europe)*, Valletta, Malta, 2025, pp. 1-5.
- [24] L. Hirth, J. Mühlenpfordt, and M. Bulkeley, "The ENTSO-E transparency platform – A review of Europe's most ambitious electricity data platform," *Appl. Energy*, vol. 225, pp. 1054-1067, Sep. 2018.

APPENDIX A

FULL-SCALE MODEL

The aggregated model presented in Subsection II-A collapses to the full-scale model when each representative time step corresponds to exactly one original time step (i.e., $\mathcal{R} = \mathcal{T}$). The solution to the full-scale GEP model serves as benchmark for the true optimum.

The full-scale decision set is defined as:

$$\mathbf{z} := \{x_g, p_{g,t}, p_{s,t}^d, p_{s,t}^c, e_t^{ns}, e_{s,t}, o_t\}_{g \in \mathcal{G}, t \in \mathcal{T}, s \in \mathcal{S}}, \quad (5)$$

with the objective function:

$$f(\mathbf{z}) := \sum_{g \in \mathcal{G}} C_g^{inv} x_g + \sum_{t \in \mathcal{T}} \left(\Delta \sum_{g \in \mathcal{G}} C_g p_{g,t} + \Delta \sum_{s \in \mathcal{S}} C_s^d p_{s,t}^d + C^{ns} e_t^{ns} - \pi_t o_t \right). \quad (6)$$

The full-scale GEP model is formulated as follows:

$$\min_{\mathbf{z} \geq 0} f(\mathbf{z}) \quad (7a)$$

$$\text{s.t.} \quad \sum_{g \in \mathcal{G}} p_{g,t} \Delta + \sum_{s \in \mathcal{S}} (p_{s,t}^d - p_{s,t}^c) \Delta + e_t^{ns} - o_t = D_t, \quad \forall t \quad (7b)$$

$$p_{g,t} \leq F_{g,t} x_g, \quad \forall g, \forall t, \quad (7c)$$

$$e_{s,t} = e_{s,t-1} + \left(\eta_s^c p_{s,t}^c - \frac{p_{s,t}^d}{\eta_s^d} \right) \Delta, \quad \forall s, \forall t, \quad (7d)$$

$$e_{s,0} = e_{s,T} = \underline{E}_s, \quad \forall s, \quad (7e)$$

$$\underline{E}_s \leq e_{s,t} \leq \overline{E}_s, \quad \forall s, \forall t, \quad (7f)$$

$$p_{s,t}^c \leq \overline{P}_s^c, \quad \forall s, \forall t, \quad (7g)$$

$$p_{s,t}^d \leq \overline{P}_s^d, \quad \forall s, \forall t, \quad (7h)$$

$$\sum_{g \in \mathcal{G}} C_g^{inv} x_g \leq \overline{B}. \quad (7i)$$

In (7), the constraints (7b) ensure the energy balance, while the constraints (7c) enforce the generation capacity limits. The storage dynamics are described by the constraints (7d)–(7f). Finally, the constraints (7g), (7h), and (7i) impose the charging, discharging, and investment limits, respectively.